

# Direct Synthesis of Diamides from Dicarboxylic Acids with Amines Using Nb<sub>2</sub>O<sub>5</sub> as a Lewis Acid Catalyst and Molecular Docking Studies as Anticancer Agents

Md. Ayub Ali,\* Ashutosh Nath, Meshkatun Jannat, and Md. Midul Islam



Cite This: *ACS Omega* 2021, 6, 25002–25009



Read Online

ACCESS |



Metrics & More

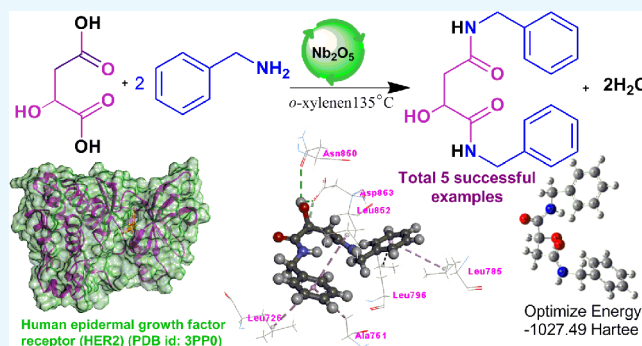


Article Recommendations



Supporting Information

**ABSTRACT:** Several Lewis and Bronsted acid catalysts were tested for the synthesis of some targeted diamides with anticancer activity from dicarboxylic acids and amines under the same reaction condition. Among those catalysts, Nb<sub>2</sub>O<sub>5</sub> showed the highest catalytic activity to the corresponding diamides. Nb<sub>2</sub>O<sub>5</sub> shows water- and base-tolerant properties for which it gives the highest yield of the synthesized products. Here, we present a novel and sustainable method for the direct synthesis of diamides with anticancer activity using a reusable heterogeneous catalyst Nb<sub>2</sub>O<sub>5</sub>. A molecular docking study was performed for all of the synthesized compounds with various therapeutical targets of cancer and found that the human epidermal growth factor receptor (HER2) has shown a significant dock score for our synthesized products. After obtaining the best pose from molecular docking, the complex is used for molecular dynamics study by running simulations for 10 ns. The root-mean-square deviations (RMSDs) of  $\alpha$  carbon atoms of all systems are analyzed to detect their stability. This method is effective for the direct synthesis of diamides as anticancer agents from dicarboxylic acids and amines using Nb<sub>2</sub>O<sub>5</sub> as a base-tolerant heterogeneous catalyst.



## 1. INTRODUCTION

The amide bond is one of the most important and studied reactions in organic chemistry.<sup>1</sup> Around 25% of drugs produced all over the world contain an amide moiety.<sup>2</sup> Therefore, amides, especially diamides, could be used as drugs against life-threatening diseases including cancer. Cancer is one of the deadliest diseases affecting humans, and every year, around 10 million cancer deaths happen worldwide.<sup>3</sup> Chemotherapy<sup>4</sup> plays a requisite role in cancer treatment, but due to severe side effects and drug resistance role, it is less satisfactory.<sup>5</sup>

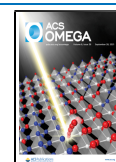
The literature survey reveals that diamide, and its derivatives are an emerging class of molecules with multiple pharmacokinetic properties.<sup>6</sup> Therefore, the development of low-toxic<sup>7</sup> and high-efficacy anticancer agents<sup>8</sup> has still been the fundamental task of medicinal chemists.<sup>9</sup> Being very much focused on this aspect by our research group, a series of diamides<sup>10</sup> have been synthesized with special emphasis given to the anticancer activity<sup>11</sup> with the establishment of the mechanism of action.

Diamide is a chemical compound containing two amide groups.<sup>12</sup> In diamide, two N atoms contain two lone pairs of electrons,<sup>13</sup> and due to the electron-withdrawing effect of carbonyl, oxygen–nitrogen centers are not basic like amine.<sup>14</sup> Several attempts were made for the synthesis of amide bonds

using Lewis acid catalysts from carboxylic acids. Lewis acid sites of the catalyst activate the carbonyl oxygen of the carboxylic acid by weakening the carbon–oxygen double bond. But the use of Lewis acid catalysts for amidation reactions has some drawbacks for this condensation reaction. Lewis acids<sup>15</sup> such as TiCl<sub>4</sub>, SiCl<sub>4</sub>, and AlCl<sub>3</sub> can decompose or deactivate the active sites of the catalyst in the presence of a small amount of water produced as byproduct or by reactant amines present in the reaction mixture. For this reason, Lewis acid-catalyzed organic reactions are usually done under complete anhydrous conditions.<sup>16</sup> Lewis acid-catalyzed amidation reactions<sup>17</sup> have additional drawbacks such as limited substrate scope, high catalyst loading, and reusability of the catalyst.<sup>18</sup> In the reaction of diamide synthesis from dicarboxylic acids with amines, water is produced as a co-product and the reaction mixture contains amines. Therefore, the presence of basic molecules (water and amines) can suppress the Lewis acidity of a catalyst.<sup>19</sup> These drawbacks can be overcome by using a

Received: August 2, 2021

Published: September 15, 2021



Lewis acid catalyst that is tolerant to basic molecules (amines and water as a byproduct) present in the reaction mixture for the amidation reactions.

To avoid the limitations of the previous method, in diamide synthesis,<sup>20</sup> a water-tolerant as well as base-tolerant<sup>21</sup> heterogeneous Lewis acid catalyst Nb<sub>2</sub>O<sub>5</sub><sup>22</sup> can be effective for the direct synthesis<sup>23</sup> of diamides from dicarboxylic acids with amines. Herein, we report the direct synthesis of some targeted diamides, which could act as anticancer agents from dicarboxylic acids with amines using Nb<sub>2</sub>O<sub>5</sub> as a base-tolerant heterogeneous Lewis acid catalyst. So far, the proposed method for the synthesis of diamide in the presence of a heterogeneous Lewis acid catalyst has not yet been reported. Herein, we report a novel, versatile, and sustainable method for the synthesis of diamides with anticancer activity.

## 2. RESULTS AND DISCUSSION

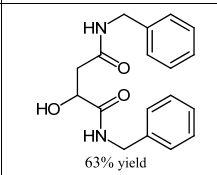
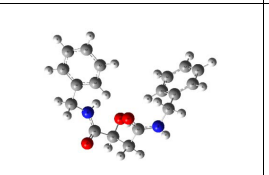
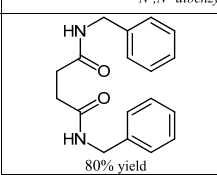
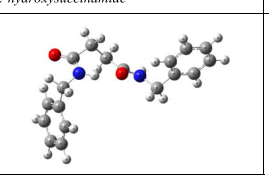
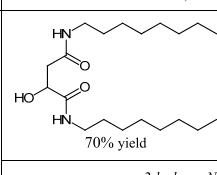
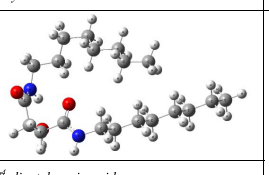
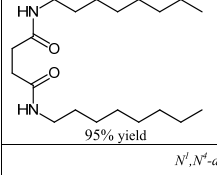
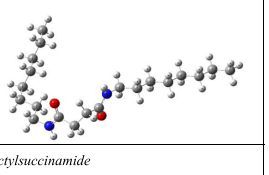
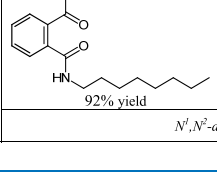
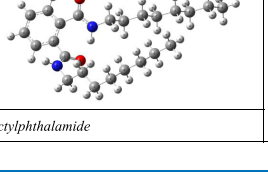
**2.1. Chemistry.** All of the diamide compounds were synthesized from dicarboxylic acids and amines in the presence of a heterogeneous Lewis acid catalyst Nb<sub>2</sub>O<sub>5</sub>. The main difficulties arise in the synthesis of diamides from dicarboxylic acids<sup>24</sup> and amines due to the production of water as a byproduct, which can suppress the Lewis acid site of the catalyst. Moreover, amide can also deactivate the catalytic activity of the Lewis acid catalyst. But as in our previous studies of amide synthesis, in this study, we also found that Nb<sub>2</sub>O<sub>5</sub> can act as water- as well as base-tolerant Lewis acid catalyst. Since the only byproduct of water is produced in this reaction, byproduct can be easily removed by a simple recrystallization reaction<sup>25</sup> with a good to high yield. Reusability of the catalyst was also performed for the reaction of succinic acid with *n*-octylamine and found that it was reusable several times with a slight loss of catalytic activity.

**2.1.1. Calcination of Catalyst.** The diamide synthesis method is divided into two steps: first, calcination of catalyst,<sup>26</sup> and second, use of the calcinated catalyst for diamide synthesis. All of the purchased catalysts were stored at room temperature. For the catalyst preparation, we used the calcination method. Commercially available Nb<sub>2</sub>O<sub>5</sub> was calcined to remove water and other possible impurities. In this method, 5 g of niobium pentoxide (Nb<sub>2</sub>O<sub>5</sub>) was taken in a crucible kept in the furnace and calcined at 500 °C for 3 h. This calcined Nb<sub>2</sub>O<sub>5</sub> was used for diamide synthesis from dicarboxylic acids with amines. Nb<sub>2</sub>O<sub>5</sub> was also prepared by calcination at 400 and 600 °C. The other catalysts such as TiO<sub>2</sub>, Al<sub>2</sub>O<sub>3</sub>, SnO<sub>2</sub>, and Cu<sub>2</sub>O were also prepared in the same method by calcination at 500 °C for 3 h.

**2.1.2. Synthesis of Diamide Derivatives.** In this work, diamides (compounds 1–5 in Table 1 and Scheme 1) were synthesized via the condensation reaction of dicarboxylic acids and amines in the presence of a heterogeneous Lewis acid catalyst. Calcinated heterogeneous Lewis acid catalysts were used as a catalyst. Typically, dicarboxylic acid and amine in a 1:2 ratio, 4 mL of *o*-xylene, and 50 mg of Nb<sub>2</sub>O<sub>5</sub> were added to the reaction vessel (RB flask). The reaction mixture was heated on a hot plate at 135 °C in a sand bath and stirred at 300 rpm. After completion of the reaction, 2-propanol (4 mL) was added to the mixture and the Nb<sub>2</sub>O<sub>5</sub> catalyst was separated from the reaction mixture by centrifugation.

Again, catalytic activity was tested by model reactions (Figure 1 and Table S1). For the model reaction, succinic acid and *n*-octylamine at 1:2 ratios were added to a round-bottom flask with 50 mg of a calcinated heterogeneous Lewis acid

**Table 1. Optimized Structures of the Synthesized Diamide Compounds 1–5**

Compound	Optimize Structure	Optimize Energy (Hartee)
1	 63% yield	
	<i>N,N'</i> -dibenzyl-2-hydroxysuccinamide	
2	 80% yield	
	<i>N,N'</i> -dibenzylsuccinamide	
3	 70% yield	
	<i>2-hydroxy-N,N'</i> -dioctylsuccinamide	
4	 95% yield	
	<i>N,N'</i> -dioctylsuccinamide	
5	 92% yield	
	<i>N,N'</i> -dioctylphthalamide	

**Scheme 1. Synthesis of Diamide Derivatives 1–5**

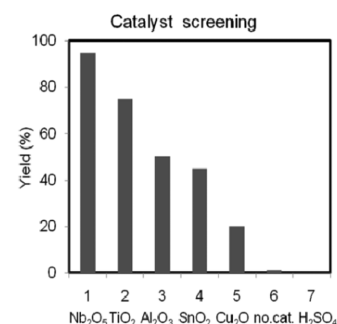
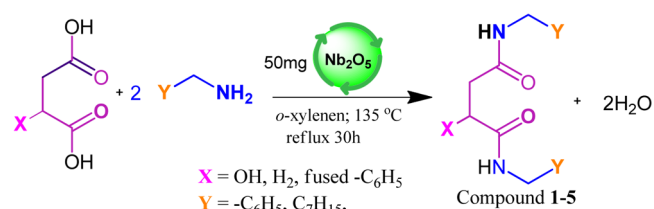


**Figure 1. Catalyst screening for model reaction.**

catalyst and 4 mL of *o*-xylene was added to the reaction mixture. This reaction mixture was heated on a hot plate at 135

°C in a sand bath for 30 h with continuous stirring at 300 rpm. The progress of the reaction was monitored by thin-layer chromatography (TLC) with *n*-hexane (2 mL) and chloroform (1 mL). Completion of the reaction was confirmed by TLC. After the completion of the reaction, the catalyst was separated from the mixture by centrifugation. The products were purified by the recrystallization separation technique. The pure diamide products were confirmed by TLC and checked by 5% NaHCO<sub>3</sub>. The synthesized pure diamide products were analyzed by ultraviolet–visible (UV–vis) spectrophotometry, Fourier transform infrared (FT-IR) spectroscopy, proton nuclear magnetic resonance (<sup>1</sup>H NMR), <sup>13</sup>C NMR, and gas chromatography–mass spectrometry (GC-MS) to determine the structure, and the catalyst was characterized by X-ray diffraction (XRD).

**2.1.2.1. Synthesis of *N*<sup>1</sup>,*N*<sup>4</sup>-Dibenzyl-2-hydroxysuccinamide 1.** White solid, yield (%): 63; mp: 146–150 °C; UV ( $\lambda_{\max}$  CHCl<sub>3</sub>): 253 nm; IR (cm<sup>-1</sup>): 3338, 3037, 2929, 1649, 1543, 1459, 1426, 1284, 1085; <sup>1</sup>H NMR (400 MHz, CDCl<sub>3</sub>):  $\delta$  7.39–7.25 (m, Ar, 10H), 6.74 (br s, 2H, -NH) 4.43–4.42 (m, 4H), 2.89–2.84 (m, 1H), 2.72–2.66 (m, 2H), 1.93 (m, -OH, 1H); <sup>13</sup>C NMR (100 MHz, CDCl<sub>3</sub>):  $\delta$  137 (2C, C=O), 128.93 (2C, Ar), 127.51 (3C, Ar), 79.08 (2C, Ar), 78.76 (1C, Ar), 76.43 (4C, Ar), 69.89 (1CH, Ar) 44.01 (1CH<sub>2</sub>, Ar), 43.50 (1CH<sub>2</sub>, Ar), 38.38 (1CH<sub>2</sub>, Ar); Calc. Mass: 312; GC-MS(CDCl<sub>3</sub>): m/e 312.

**2.1.2.2. Synthesis of *N*<sup>1</sup>,*N*<sup>4</sup>-Dibenzylsuccinamide 2.** White solid, yield (%): 80; mp: 212–215 °C; UV ( $\lambda_{\max}$  CHCl<sub>3</sub>): 340, 258 nm; IR (cm<sup>-1</sup>): 3298, 3086, 2923, 1635, 1555, 1455, 1338, 1218, 1029; <sup>1</sup>H NMR (400 MHz, CDCl<sub>3</sub>):  $\delta$  7.35–7.28 (m, Ar, 10H), 6.20 (br s, 2H, -NH) 4.46 (s, 4H), 2.63 (s, 4H); <sup>13</sup>C NMR (100 MHz, CDCl<sub>3</sub>):  $\delta$  165 (2C, C=O), 128.72 (6C, Ar), 127.72 (4C, Ar), 127.52 (2C, Ar), 43.72 (2C), 41.50 (2C); Calc. Mass: 296; GC-MS(CDCl<sub>3</sub>): m/e 296.

**2.1.2.3. Synthesis of 2-Hydroxy-*N*<sup>1</sup>,*N*<sup>4</sup>-dioctylsuccinamide 3.** White solid, yield (%): 70; mp: 150–152 °C; UV ( $\lambda_{\max}$  CHCl<sub>3</sub>): 383 nm; IR (cm<sup>-1</sup>): 3295, 3102, 2921, 2852, 1645, 1567, 1436, 1334, 1287, 1189; <sup>1</sup>H NMR (400 MHz, CDCl<sub>3</sub>):  $\delta$  7.06 (br s, 1H, -NH), 6.37 (br s, 1H, -NH), 4.38–4.36 (m, 1H, -OH), 3.29–3.22 (m, 4H), 2.80–2.76 (m, 1H), 2.66–2.60 (m, 2H), 1.53–1.49 (m, 4H), 1.29–1.28 (m, 20H), 0.91–0.88 (t, *J* = 6.40 Hz, 6H); <sup>13</sup>C NMR (100 MHz, CDCl<sub>3</sub>):  $\delta$  173.67 (1C, C=O), 172.67 (1C, C=O), 68.50 (1CH<sub>2</sub>, Ar), 40.21 (1CH<sub>2</sub>), 39.58 (1CH<sub>2</sub>), 38.40 (1CH), 31.81 (2CH<sub>2</sub>), 29.21 (4CH<sub>2</sub>), 26.88 (2CH<sub>2</sub>), 22.66 (2CH<sub>2</sub>), 14.12 (3CH<sub>2</sub>). Calc. Mass: 356; GC-MS(CDCl<sub>3</sub>): m/e 356.

**2.1.2.4. Synthesis of *N*<sup>1</sup>,*N*<sup>4</sup>-Dioctylsuccinamide 4.** White solid, yield (%): 95; mp: 171–174 °C; UV ( $\lambda_{\max}$  CHCl<sub>3</sub>): 340 nm; IR (cm<sup>-1</sup>): 3304, 3091, 2922, 2852, 1633, 1546, 1426, 1349, 1220, 1160; <sup>1</sup>H NMR (400 MHz, CDCl<sub>3</sub>):  $\delta$  6.20 (br s, 2H, -NH), 3.27–3.22 (m, 4H), 2.57 (s, 4H), 1.67 (m, 4H), 1.51–1.49 (m, 4H), 1.29–1.28 (m, 16H), 0.91–0.88 (t, *J* = 6.40 Hz, 6H); <sup>13</sup>C NMR (100 MHz, CDCl<sub>3</sub>):  $\delta$  172 (2C, C=O), 39.75 (2C), 31.98–31.81 (2C, C-N), 29.52–29.21 (2C), 26.92 (2C), 22.65 (8C), 14 (2C); Calc. Mass: 340; GC-MS(CDCl<sub>3</sub>): m/e 340, 297, 242, 212, 156, 100.

**2.1.2.5. Synthesis of *N*<sup>1</sup>,*N*<sup>2</sup>-Dioctylphthalamide 5.** White solid, yield (%): 92; mp: 127–130 °C; UV ( $\lambda_{\max}$  CHCl<sub>3</sub>): 242 nm; IR (cm<sup>-1</sup>): 3238, 3078, 2929, 2856, 1627, 1544, 1457, 1426, 1317, 1155, 1166; <sup>1</sup>H NMR (400 MHz, CDCl<sub>3</sub>):  $\delta$  7.60–7.58, 7.47–7.45 (m, Ar, 4H), 6.78 (br s, 2H, -NH), 3.41–3.36 (m, 4H), 1.78 (m, 4H), 1.62–1.55 (m, 4H), 1.34–1.29 (m, 16H), 0.91–0.86 (t, *J* = 6.40 Hz, 6H); <sup>13</sup>C NMR

(100 MHz, CDCl<sub>3</sub>):  $\delta$  169.24 (2C, C=O), 134.67 (1C, Ar), 133.85 (1C, Ar), 132.22 (1CH, Ar), 130.17 (2CH, Ar), 128.37 (3CH, Ar), 123.17 (1CH, Ar), 40.35 (1CH<sub>2</sub>, Ar), 31.83 (2CH<sub>2</sub>, Ar), 29.31 (3CH<sub>2</sub>), 27.00 (1CH<sub>2</sub>), 26.89 (2CH<sub>2</sub>), 22.66 (2CH<sub>2</sub>), 14.10 (1CH<sub>2</sub>); Calc. Mass: 388; GC-MS(CDCl<sub>3</sub>): m/e 388.

**2.2. Effect of the Calcination Temperature of Nb<sub>2</sub>O<sub>5</sub> for Model Reaction.** All of the purchased catalysts were stored at room temperature. For the catalyst preparation, we used the calcination method.<sup>27</sup> Commercially available Nb<sub>2</sub>O<sub>5</sub> was calcined to remove water and other possible impurities. In this method, 5 g of niobium pentoxide (Nb<sub>2</sub>O<sub>5</sub>) was taken in a crucible and kept in a furnace at 500 °C for 3 h. After completing calcination, Nb<sub>2</sub>O<sub>5</sub> was used for diamide synthesis. Nb<sub>2</sub>O<sub>5</sub> was also prepared by calcination at 400 and 600 °C. The effect of calcination temperature was checked for the reaction of succinic acid with *n*-octylamine, and it was found that Nb<sub>2</sub>O<sub>5</sub> shows the highest catalytic activity when it was calcined at 500 °C for 3 h (95% yield of the product) (Figure 2 and Table S2).

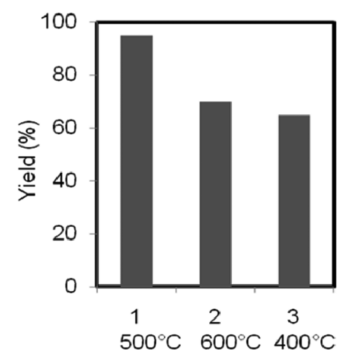


Figure 2. Effect of calcination temperature for model reaction.

**2.3. Lewis Acidity of Nb<sub>2</sub>O<sub>5</sub>.** In our previous report,<sup>15</sup> we showed that Nb<sub>2</sub>O<sub>5</sub> was used for the activation of the C=O bond of carboxylic acid by weakening the C=O bond. It was also shown that for the amide bond formation reaction by Nb<sub>2</sub>O<sub>5</sub>, mainly Lewis acid sites (exposed Nb<sup>5+</sup> cations) act as catalyst. It was also reported that Lewis acid sites of Nb<sub>2</sub>O<sub>5</sub>, TiO<sub>2</sub>, and Al<sub>2</sub>O<sub>3</sub> is 0.058, 0.083, and 0.148 mmol g<sup>-1</sup>, respectively. Therefore, the main reason of the higher catalytic activity of Nb<sub>2</sub>O<sub>5</sub> (Figure 1) is not the number of Lewis acid sites but the water- and base-tolerant property of Nb<sub>2</sub>O<sub>5</sub>. Besides, the highest surface area (54 m<sup>2</sup>g<sup>-1</sup>) of Nb<sub>2</sub>O<sub>5</sub> was found at 500 °C. Therefore, Nb<sub>2</sub>O<sub>5</sub> calcined at 500 °C showed the highest catalytic activity (Figure 2).

**2.4. Base-Tolerant Catalysis of Nb<sub>2</sub>O<sub>5</sub> for Amidation.** We have also analyzed the effect of base (water and pyridine) on Nb<sub>2</sub>O<sub>5</sub> and TiO<sub>2</sub> for the amidation of succinic acid and *n*-octylamine by adding water and pyridine in the reaction system (Table S3 and Figure S3). To compare the base-tolerant properties of Nb<sub>2</sub>O<sub>5</sub> and TiO<sub>2</sub>, we measured the yield of the diamide in the model reaction for 30 h with Nb<sub>2</sub>O<sub>5</sub> or TiO<sub>2</sub> under the reflux conditions in the presence of 1 and 0.5 mmol of basic additives, H<sub>2</sub>O and pyridine. The negative effects of the additives were lower for Nb<sub>2</sub>O<sub>5</sub> than TiO<sub>2</sub>. This suggests that the active site (Nb<sup>5+</sup> Lewis acid site) interacts preferentially with the reactant (dicarboxylic acid) in the presence of basic molecules. Summarizing the above results, we can conclude that the Lewis acid site of Nb<sub>2</sub>O<sub>5</sub> has higher

tolerance to basic molecules than TiO<sub>2</sub> conventional solid Lewis acid.

**2.5. Reusability of Nb<sub>2</sub>O<sub>5</sub>.** We have studied the reusability of Nb<sub>2</sub>O<sub>5</sub> for the model reaction after the reaction catalyst was separated from the mixture by centrifugation, followed by washing with acetone and drying at 90 °C for 3 h. The recovered catalyst was reused four times with a slight decrease in product yield (Figure 3). The initial rates for the first cycle

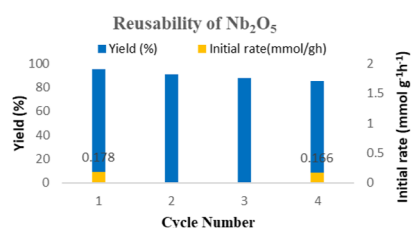


**Figure 3.** Reusability of Nb<sub>2</sub>O<sub>5</sub> for the synthesis of N<sup>1</sup>,N<sup>4</sup>-dioctylsuccinamide from succinic acid (1 mmol) and *n*-octylamine (2 mmol) under *o*-xylene reflux condition for 30 h.

(0.178 mmol g<sup>-1</sup> h<sup>-1</sup>) and fourth cycle (0.166 mmol g<sup>-1</sup> h<sup>-1</sup>) also showed a slight decrease in the rate of the model reaction for reusability study.

**2.6. Characterization of Catalyst.** X-ray diffraction (XRD) patterns of calcinated niobium pentoxide at 500 °C before being used in the reaction and after four cycles in the powder state are shown in Figures S8 and S9, respectively. The XRD data showed that the phase of Nb<sub>2</sub>O<sub>5</sub> does not show any change even after four cycles. Therefore, Nb<sub>2</sub>O<sub>5</sub> acts as a reusable heterogeneous Lewis acid catalyst for diamide synthesis from dicarboxylic acids and amines.

**2.7. Frontier Molecular Orbital Studies.** The energy levels of the molecular orbitals order highest occupied molecular orbital (HOMO) and lowest unoccupied molecular orbital (LUMO)<sup>28</sup> amide derivatives give information on the possible electronic transition. We analyzed the electrophilic and nucleophilic attraction region in a molecule by the HOMO and LUMO, as shown in Figure S10. For the chemical reactivity calculation, the LUMO–HOMO gap is the most important parameter. The lower LUMO–HOMO gap indicates high reactivity. The data of HOMO, LUMO for different energy levels and chemical reactivity<sup>29</sup> are listed in Table 2.  $E_{\text{gap}} = (E_{\text{LUMO}} - E_{\text{HOMO}}) \approx \text{IP} - \text{EA}$ ;  $I = -E_{\text{HOMO}}$ ,  $\text{EA} = -E_{\text{LUMO}}$ ;  $\mu = -(I + A)/2$ ;  $\eta = (I - A)/2$ ;  $S = 1/\eta$ ;  $\chi = (I + A)/2$  and  $\omega = \mu^2/2\eta$ .

**Table 2.** Chemical Reactivity of Amide<sup>a</sup>

compounds	1	2	3	4	5
$E_{\text{HOMO}}$ (eV)	-0.22258	-0.21995	-0.21675	-0.22745	-0.21943
$E_{\text{LUMO}}$ (eV)	-0.00180	-0.01089	0.02628	0.03504	-0.04288
energy gap $\Delta E$ (eV)	0.22078	0.20906	0.24303	0.26249	0.17655
ionization potential IP (eV)	0.22258	0.21995	0.21675	0.22745	0.21943
electron affinity EA (eV)	0.00180	0.01089	-0.02628	-0.03504	0.04288
electronegativity (eV)	0.11219	0.11542	0.095235	0.096205	0.131155
chemical potential $\mu$	-0.11219	-0.11542	-0.09524	-0.09621	-0.13116
chemical hardness $\eta$ (eV)	0.11039	0.10453	0.121515	0.131245	0.088275
softness chemical hardness $S$ (eV) <sup>-1</sup>	4.529396	4.783316	4.114718	3.809669	5.664118
electrophilicity index $\omega$ (eV)	0.05701	0.063722	0.037319	0.03526	0.097432

<sup>a</sup>From the above calculations, five amide derivatives compounds 1–5 have good chemical reactivity and are soft, while compound 1 shows the lowest energy gap. With the greater value of softness, we can introduce compounds 1 and 2 that show higher biological activity.

**2.8. Molecular Docking Studies.** For better understanding, it has been observed that the structure–activity relationships and molecular docking study<sup>30</sup> of the compounds 1–5 with various therapeutic targets of cancer showed that human epidermal growth factor receptor (HER2)<sup>31</sup> has shown a significant dock score, as presented in Table 3. All of the compounds show binding energy and binding affinity, whereas the majority of the compounds show moderate scores with another target, i.e., EGFR,<sup>32</sup> VEGFR2,<sup>33</sup> and Aromatase.<sup>34</sup>

The results of docking, binding affinity, and binding energy calculations against HER2 compounds 1 and 2 have shown the highest dock score of -9.1 kcal/mol. Compound 1 has shown three, five, one, and two H bonds with active site amino acids with PDB IDs 3PP0, 4AG8, 4EQM, and 4HJO and dock scores of -9.1, -8.5, -7.2, and -8.5 kcal/mol, respectively. The -OH group of compound 1 acts as a H-bond acceptor, and its oxygen atom is formed between three H bonds, one with OH of ASN850 (bond length, 2.79 Å) and two with OH of ASP863 (bond lengths 2.72 and 2.73 Å) with Human epidermal growth factor receptor (HER2) (PDB id: 3PP0). The docking results revealed that amino acids ASN850 and ASP863 located in the binding pocket of protein played important roles. Similarly, compound 2 has shown one, zero, two, and one H bonds with docking scores of -9.1, -8.6, -7.1, and -7.6 kcal/mol with PDB IDs 3PP0, 4AG8, 4EQM, and 4HJO, respectively. The complex act as a H-bond acceptor, and its oxygen and hydrogen atoms have formed two H bonds, one with C=O of THR766 and the other with OH of ASP831 with 2.32 and 2.05 Å against Epidermal growth factor receptor (EGFR) (PDB id: 4HJO). Based on the characterization of protein–ligand interactions,<sup>35</sup> it is evident that compounds 1 and 2 played a key role in forming H-bond interactions in both in silico studies. The docking calculation of all of the compounds (1–5) was also included in Table S4 and Figure S11a–d in the Supporting Information.

**2.9. Molecular Dynamic (MD) Simulation Studies.** After obtaining the best pose from molecular docking, the complex is used for molecular dynamics<sup>36</sup> study by running simulations for 10 ns. The root-mean-square deviation (RMSD)<sup>37</sup> of  $\alpha$  carbon atoms of all systems is analyzed to detect their stability. We observed from Figure 5 that two complexes exhibit the lowest RMSD than other complexes. The MD simulation of compound 1 against 3PP0 and 4HJO protein demonstrates the lowest RMSD value than compound 2 + 3PP0 complex, which indicates its greater stability and

Table 3. Docking Scores of Compounds 1–5

compounds	Human epidermal growth factor receptor (HER2) (PDB id: 3PP0)	Vascular endothelial growth factor receptor 2 (VEGFR2) (PDB id: 4AG8)	Human placental Aromatase, Cytochrome P 450 (PDB id: 4EQM)	Epidermal growth factor receptor (EGFR) (PDB id: 4HJO)
1	−9.1	−8.5	−7.2	−8.5
2	−9.1	−8.6	−7.1	−7.6
3	−7.0	−6.6	−5.2	−6.3
4	−5.5	−6.9	−5.1	−7.7
5	−8.3	−7.8	−5.8	−5.1

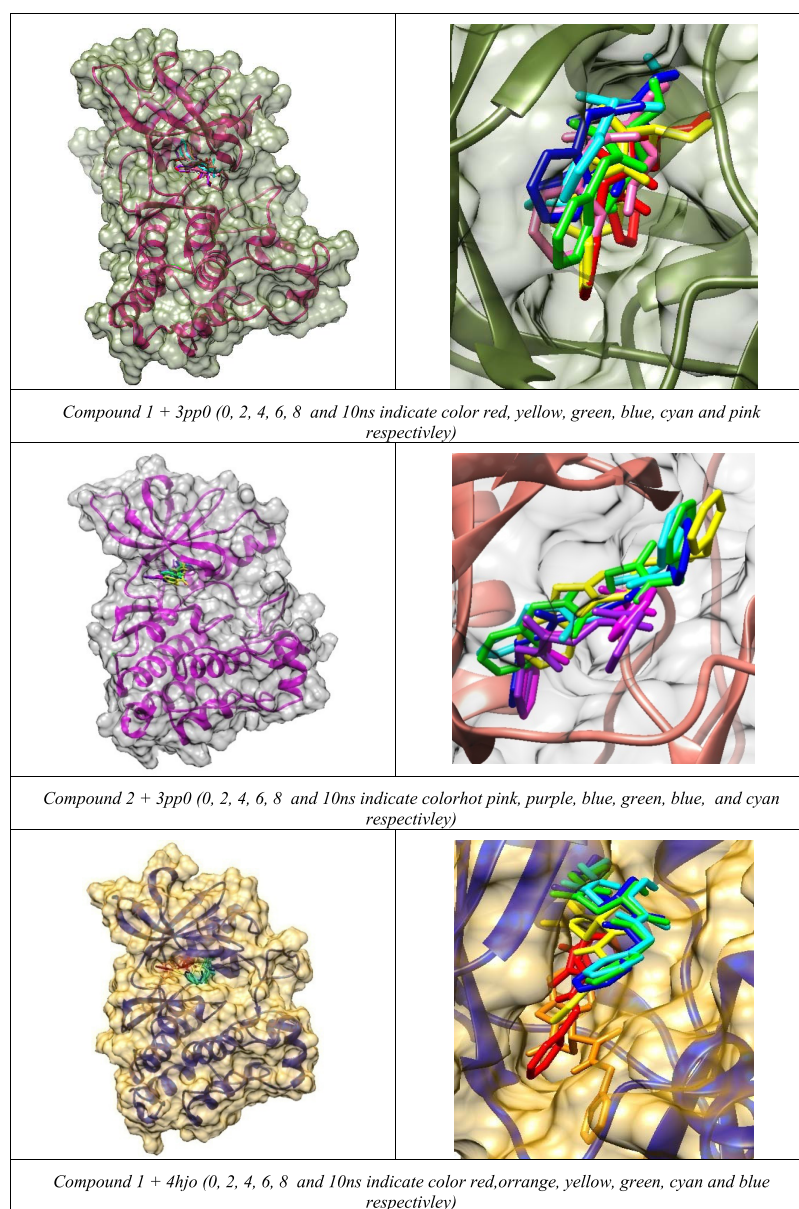


Figure 4. 2 ns snapshots of MD simulations.

keeps in the pocket of proteins. As a result, the compound has to be considered as a drug.

The root-mean-square fluctuation (RMSF)<sup>38</sup> helps to understand the region of protein that is being fluctuated during the MD simulation, and the flexibility of per residue is computed to get better acumen on the extent to which the binding of ligand affects the protein flexibility.

Analysis of RMSD and RMSF of compounds 1 and 2 against 3PP0 and 4HJO complexes is also shown in Figure 5, and 2 ns

snapshots are shown in Figure 4. Finally, we found the stability and protein interaction with amide molecules from the height range of MD study in Figure 5, this data provides information about drug activity of amide molecules.

**2.10. Toxicity Risk Assessment Screening.** Toxic properties such as irritant, mutagenic, tumorigenic, and reproductive effects were screened for the diamide derivatives (1–5) using Molinspiration, admetsar2, and Osiris server (<https://openmolecules.org/propertyexplorer/applet>).

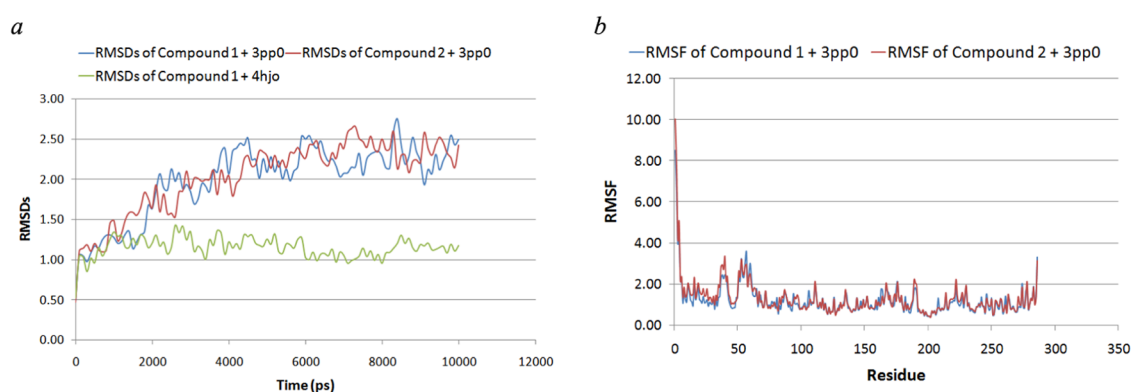


**Figure 5.** Analysis of RMSDs and RMSFs of selected three complexes with protein at 10 ns MD simulations. (a) Root-mean-square deviations (RMSDs) of the 3PP0 and (b) root-mean-square fluctuations (RMSFs) of the 3PP0 and 4HJO.

**Table 4.** Toxicity Risk Assessment Screening of Compounds (1–5) Computed with MOLINSPIRATION and OSIRIS Server

compound	clog <i>P</i>	solubility	drug-likeness	drug score	mutagenic	tumorigenic	irritant	reproductive effect
1	1.06	−2.7	1.68	0.83	no	no	no	no
2	2.08	−3.1	0.3	0.69	no	no	no	no
3	4.48	−3.9	−1728	0.33	no	no	no	no
4	5.51	−4.3	−17.58	0.27	no	no	no	no
5	7.26	−5.74	−20.32	0.16	no	no	no	no

**Table 5.** ADME Properties of Compounds (1–5) Computed through MOE QSAR Descriptor Module

compound	log <i>P</i> ( <i>o/w</i> ) < 5	MW < 500	TPSA < 140	HBA < 10	HBD < 5	nRotB < 10	molar refractivity
1	0.95	312.37	78.42	3	3	7	87.10
2	1.86	296.37	58.20	2	2	7	85.93
3	5.07	356.55	78.42	3	3	17	105.42
4	5.98	340.55	58.20	2	2	17	104.26
5	7.19	388.60	58.20	2	2	16	119.73

html, <https://www.molinspiration.com/>, <http://www.swissadme.ch/index.php>). The server is inbuilt with a list of about 5300 distinct substructure fragments created by 15 000 commercially available fragments with reported drug score and drug-likeness. Drug scores associated with drug-likeness, clog *P*, molecular weight, and toxicity risks as a total value may be used to judge the overall potential to qualify it as a drug. The toxicity screening of compounds 1 and 2 showed no risk of mutagenic, tumorigenic, irritant, and reproductive toxicity (Table 4).

**2.11. Theoretical Evolution of ADME Properties.** The bioavailability of diamide derivatives (1–5) was accessed through ADME (adsorption, distribution, metabolism, and excretion) using admetsar2 online server (<http://lmm.d.ecust.edu.cn/admetsar2/>). To explore the druglike properties of compounds (1–5), the lipophilicity, expressed as the octanol/water partition coefficient and here called log *P*(*o/w*), as well as other theoretical calculations such as molecular size, topological polar surface area (TPSA), number of hydrogen-bond acceptors and donors, and the number of rotatable bonds, were calculated (Table 5).

### 3. CONCLUSIONS

In the present work, we showed that Nb<sub>2</sub>O<sub>5</sub> acts as an effective, base-tolerant, reusable, and commercially available heterogeneous Lewis acid catalyst for the direct synthesis of diamides from dicarboxylic acids and amines. This method offers several advantages, including facile reaction conditions as well as simple experimental and product isolations procedures.

Herein, a series of five compounds were synthesized and characterized with good yields. This work also focused on the anticancer activity of chemically diverse diamide-containing compounds 1 and 2 significantly exhibiting inhibitory activity against four cancer cell lines, viz., lung (A549), breast (MCF-7), colon (HT-29), and melanoma (A375). MD simulations showed that compounds 1 and 2 are located in the pocket of the anticancer cell. As a result, it can play an effective role as a drug in any biological system. In addition, AMDET studies have been performed for their side effects, suggesting that not all drugs have anticancer activity.

### 4. EXPERIMENTAL SECTION

**4.1. General.** All of the chemicals, catalysts, and solvents were purchased from Sigma-Aldrich (Germany) and TCI (Japan) and were used without further purification. TLC was performed on precoated TLC plates (silica gel 60, Merck).

**4.2. Synthesis.** After optimization of reaction condition, dicarboxylic acids and amines (1:2 ratio) were placed in a round-bottom flask with the catalyst Nb<sub>2</sub>O<sub>5</sub> (50 mg). Then, *o*-xylene solvent (4 mL) was added to the flask and the mixture was heated at the *o*-xylene reflux temperature with continuous stirring (400 rpm). After completion of the reaction, the product was separated from the reaction mixture by centrifugation. Then, the product was dried and recrystallized for purification. Finally, the pure product was analyzed by UV–vis, FT-IR, NMR, and GC-MS spectroscopic techniques.

**4.3. Spectroscopic Measurements.** <sup>1</sup>H and <sup>13</sup>C NMR spectra were recorded in a ZEOL-400 NMR spectrometer and

a Bruker 600 NMR spectrometer. UV–vis, FT-IR, and GC-MS spectra were recorded in a Shimadzu spectrometer.

**4.5. Computational Methods.** Optimization of the structure and calculation of vibrational frequency were done by density functional theory (DFT) calculations.<sup>39</sup> The B3LYP functional<sup>40</sup> was used with a 6-31++G(d,p) basis set.<sup>41</sup> Gaussian 16W<sup>42</sup> and GaussView 6.0.16 packages were used for optimization and visualizations. All computational analyses were carried out on a Windows platform running on an HP Probook Intel Core i3 processor and 8 GB of RAM.

**4.6. Protein Structure.** The crystal structure of the protein was taken from the RCSB Protein Databank<sup>43</sup> (PDB ID: 3PP0, 4HJO, 4AG8, and 4EQM). Before the protein preparation process, all of the water molecules and heteromolecules attached with the structures, i.e., RNA, were removed from the original crystal structure of four proteins. Hydrogen atoms were added, and the geometry of all of the heterogroups was corrected.

**4.7. Molecular Docking.** Protein–ligand docking studies are one of the main challenging aspects of computer-aided drug design. Docking of the diamide derivative compounds 1–5 was performed in AutoDock 4.00 Vina.<sup>44</sup> Since those programs are based on different methods for ligand placement and scoring, using both programs simultaneously normally increases the change of generation of the correct ligand pose. Vina includes an iterated local search global optimizer as a searching method and a combination of knowledge-based and empirical potentials as a scoring function. After docking, the best four conformations of the substrate were taken for the next step of the molecular dynamics study.

**4.8. Molecular Dynamic (MD) Simulations.** Four selected diamide complexes were used for MD simulation. MD simulation was performed by the YASARA program.<sup>45</sup> The simulation was performed in an explicit water environment, the model was simulated at 25 °C and a constant pressure using AMBER14 force field<sup>46</sup> under periodic cell boundary condition. Finally, a 10 ns MD simulation was performed at 25 °C and 1 atm pressure without positional restraint for both the systems. The RMSD and RMSF values were examined for each simulation. An HP Probook 6460b laptop was used for all of the prediction and simulation studies.

## ■ ASSOCIATED CONTENT

### SI Supporting Information

The Supporting Information is available free of charge at <https://pubs.acs.org/doi/10.1021/acsomega.1c04069>.

Methodology; calcination of catalyst, reaction scheme, characterization of the products by UV–vis, FT-IR, and NMR spectroscopy; catalyst screening, solvent screening, characterization of catalyst by XRD; base-tolerant properties of catalyst Nb<sub>2</sub>O<sub>5</sub>, and comparison with other Lewis acid catalysts; data of HOMO, LUMO, and molecular docking; spectra of different spectroscopic techniques; and brief descriptions (PDF)

## ■ AUTHOR INFORMATION

### Corresponding Author

Md. Ayub Ali – *Catalysis and Organic Synthesis Laboratory, Department of Chemistry, Bangladesh University of Engineering and Technology, Dhaka 1000, Bangladesh*;  
ORCID: <https://orcid.org/0000-0002-0915-7771>; Email: [shuvro70@chem.buet.ac.bd](mailto:shuvro70@chem.buet.ac.bd)

## Authors

**Ashutosh Nath** – *Computational Research for Material Science and Drug Discovery Laboratory, Department of Chemistry, Bangladesh University of Engineering and Technology, Dhaka 1000, Bangladesh*; Present Address: Department of Chemistry, University of Massachusetts Boston, Boston, Massachusetts 02125, United States; ORCID: <https://orcid.org/0000-0001-8302-0493>

**Meshkatun Jannat** – *Catalysis and Organic Synthesis Laboratory, Department of Chemistry, Bangladesh University of Engineering and Technology, Dhaka 1000, Bangladesh*

**Md. Midul Islam** – *Catalysis and Organic Synthesis Laboratory, Department of Chemistry, Bangladesh University of Engineering and Technology, Dhaka 1000, Bangladesh*

Complete contact information is available at:

<https://pubs.acs.org/10.1021/acsomega.1c04069>

## Notes

The authors declare no competing financial interest.

## ■ ACKNOWLEDGMENTS

The authors are grateful to the Bangladesh University of Engineering and Technology (BUET), Dhaka, Dhaka-1000, Bangladesh, for all kinds of experimental and financial supports.

## ■ REFERENCES

- (1) Valeur, E.; Bradley, M. Amide bond formation: beyond the myth of coupling reagents. *Chem. Soc. Rev.* **2009**, *38*, 606–631.
- (2) Almarsson, Ö.; Zaworotko, M. J. Crystal engineering of the composition of pharmaceutical phases. Do pharmaceutical co-crystals represent a new path to improved medicines? *Chem. Commun.* **2004**, *17*, 1889–1896.
- (3) Wagner, K.-H.; Brath, H. A global view on the development of non communicable diseases. *Preventive medicine* **2012**, *54*, S38–S41.
- (4) Sternberg, C. N.; Donat, S. M.; et al. Chemotherapy for bladder cancer: treatment guidelines for neoadjuvant chemotherapy, bladder preservation, adjuvant chemotherapy, and metastatic cancer. *J. Urol.* **2007**, *69*, 62–79.
- (5) Li, L.; Zhang, Z.; Luo, F.; et al. Management of drug-resistant spinal tuberculosis with a combination of surgery and individualised chemotherapy: a retrospective analysis of thirty-five patients. *Int. Orthop.* **2012**, *36*, 277–283.
- (6) Neralagundi, H. S.; Begum, A. B.; Prabhakar, B.; Khanum, S. A. Design and synthesis of diamide-coupled benzophenones as potential anticancer agents. *Eur. J. Med. Chem.* **2016**, *115*, 342–351.
- (7) Moore, D. R. J.; Caux, P.-Y. Estimating low toxic effects. *Environ. Toxicol. Chem.* **1997**, *16*, 794–801.
- (8) Zafir-Lavie, I.; Michaeli, Y.; Reiter, Y. Novel antibodies as anticancer agents. *Oncogene* **2007**, *26*, 3714–3733.
- (9) Walters, W. P.; Green, J.; Weiss, J. R.; Murcko, M. A. What do medicinal chemists actually make? A 50-year retrospective. *J. Med. Chem.* **2011**, *54*, 6405–6416.
- (10) Hirpara, K. V.; Aggarwal, P.; Mukherjee, A. J.; Joshi, N.; Burman, A. C. Quercetin and its derivatives: synthesis, pharmacological uses with special emphasis on anti-tumor properties and prodrug with enhanced bio-availability. *Anti-Cancer Agents Med. Chem.* **2009**, *9*, 138–161.
- (11) Kuttan, R.; Bhanumathy, P.; Nirmala, K.; George, M. Potential anticancer activity of turmeric (*Curcuma longa*). *Cancer Lett.* **1985**, *29*, 197–202.
- (12) Jancik, V.; Pineda, L. W.; et al. Preparation of Monomeric [LAl(NH<sub>2</sub>)<sub>2</sub>]<sup>2+</sup>—A Main-Group Metal Diamide Containing Two Terminal NH<sub>2</sub> Groups. *Angew. Chem., Int. Ed.* **2004**, *43*, 2142–2145.

- (13) Brzezinski, B.; Zundel, G. Intramolecular easily polarizable hydrogen bonds in diamides of succinic and *o*-phthalic acid. *Chem. Phys. Lett.* **1979**, *61*, 315–318.
- (14) Hay, R. W.; Govan, N.; Perotti, A.; Carugo, O. Copper (II), nickel (II) and palladium (II) complexes of the diamide ligand N, N'-bis (2-carbamoyl) ethylenediamine (H2L) and the crystal structure of the carbonyl-oxygen-bonded copper (II) complex [Cu (H2L)](ClO4) 2. *Transition Met. Chem.* **1997**, *22*, 389–394.
- (15) Hakim Siddiki, S. M. A.; Rashed, M. N.; et al. Lewis acid catalysis of Nb2O5 for reactions of carboxylic acid derivatives in the presence of basic inhibitors. *ChemCatChem* **2019**, *11*, 383–396.
- (16) Fringuelli, F.; Pizzo, F.; Vaccaro, L. Lewis-acid catalyzed organic reactions in water. The case of AlCl3, TiCl4, and SnCl4 believed to be unusable in aqueous medium. *J. Org. Chem.* **2001**, *66*, 4719–4722.
- (17) Ali, M. A.; Siddiki, S.; Onodera, W.; Kon, K.; Shimizu, K.-i. Amidation of carboxylic acids with amines by Nb2O5 as a reusable Lewis acid catalyst. *ChemCatChem* **2015**, *7*, 3555–3561.
- (18) Yadav, M.; Singh, V.; Sharma, Y. C. Methyl transesterification of waste cooking oil using a laboratory synthesized reusable heterogeneous base catalyst: Process optimization and homogeneity study of catalyst. *Energy Convers. Manage.* **2017**, *148*, 1438–1452.
- (19) Bah, J.; Franzén, J. Carbocations as Lewis Acid Catalysts in Diels–Alder and Michael Addition Reactions. *Chem. - Eur. J.* **2014**, *20*, 1066–1072.
- (20) Crich, D.; Sasaki, K.; Rahaman, M. Y.; Bowers, A. A. One-pot syntheses of dissymmetric diamides based on the chemistry of cyclic monothioanhydrides. Scope and limitations and application to the synthesis of glycodipeptides. *J. Org. Chem.* **2009**, *74*, 3886–3893.
- (21) Ali, M. A.; Siddiki, S. H.; Kon, K.; Hasegawa, J.; Shimizu, K. Versatile and sustainable synthesis of cyclic imides from dicarboxylic acids and amines by Nb2O5 as a base-tolerant heterogeneous Lewis acid catalyst. *Chem. - Eur. J.* **2014**, *20*, 14256–14260.
- (22) Ali, M. A.; Siddiki, S. H.; Kon, K.; Shimizu, K. A heterogeneous niobium (V) oxide catalyst for the direct amidation of esters. *ChemCatChem* **2015**, *7*, 2705–2710.
- (23) Ali, M. A.; Moromi, S. K.; Touchy, A. S.; Shimizu, K. Direct Synthesis of Cyclic Imides from Carboxylic Anhydrides and Amines by Nb2O5 as a Water-Tolerant Lewis Acid Catalyst. *ChemCatChem* **2016**, *8*, 891–894.
- (24) Lanigan, R. M.; Sheppard, T. D. Recent developments in amide synthesis: Direct amidation of carboxylic acids and transamidation reactions. *Eur. J. Org. Chem.* **2013**, *2013*, 7453–7465.
- (25) Roberts, W.; Boden, H.; Ahlblom, B. Dynamic recrystallization kinetics. *Met. Sci.* **1979**, *13*, 195–205.
- (26) Chai, S.-H.; Wang, H.-P.; Liang, Y.; Xu, B.-Q. Sustainable production of acrolein: Gas-phase dehydration of glycerol over Nb2O5 catalyst. *J. Catal.* **2007**, *250*, 342–349.
- (27) Liu, Y.; Lin, C.; Wu, Y. Characterization of red mud derived from a combined Bayer Process and bauxite calcination method. *J. Hazard. Mater.* **2007**, *146*, 255–261.
- (28) Pereira, F.; Xiao, K.; Latino, D. A.; Wu, C.; Zhang, Q.; Aires-de-Sousa, J. Machine learning methods to predict density functional theory B3LYP energies of HOMO and LUMO orbitals. *J. Chem. Inf. Model.* **2017**, *57*, 11–21.
- (29) Chermette, H. Chemical reactivity indexes in density functional theory. *J. Comput. Chem.* **1999**, *20*, 129–154.
- (30) Yang, X.-H.; Xiang, L.; et al. Synthesis, biological evaluation, and molecular docking studies of 1, 3, 4-thiadiazol-2-amide derivatives as novel anticancer agents. *Bioorg. Med. Chem.* **2012**, *20*, 2789–2795.
- (31) Fendly, B. M.; Winget, M.; et al. Characterization of murine monoclonal antibodies reactive to either the human epidermal growth factor receptor or HER2/neu gene product. *Cancer Res.* **1990**, *50*, 1550–1558.
- (32) Nicholson, R. I.; Gee, J. M. W.; Harper, M. E. EGFR and cancer prognosis. *Eur. J. Cancer* **2001**, *37*, 9–15.
- (33) Sawamiphak, S.; Seidel, S.; Essmann, C. L.; Wilkinson, G. A.; Pitulescu, M. E.; Acker, T.; Acker-Palmer, A. Ephrin-B2 regulates VEGFR2 function in developmental and tumour angiogenesis. *Nature* **2010**, *465*, 487–491.
- (34) Smith, I. E.; Dowsett, M. Aromatase inhibitors in breast cancer. *N. Engl. J. Med.* **2003**, *348*, 2431–2442.
- (35) Muegge, I.; Martin, Y. C. A general and fast scoring function for protein–ligand interactions: a simplified potential approach. *J. Med. Chem.* **1999**, *42*, 791–804.
- (36) Sarkar, M.; Nath, A.; Kumer, A.; Mallik, C.; Akter, F.; Moniruzzaman, Md.; Ali, MdA. Synthesis, molecular docking screening, ADMET and dynamics studies of synthesized 4-(4-methoxyphenyl)-8-methyl-3,4,5,6,7,8-hexahydroquinazolin-2(1H)-one and quinazolinone derivatives. *J. Mol. Struct.* **2021**, *1244*, No. 130953.
- (37) Kuzmanic, A.; Zagrovic, B. Determination of ensemble-average pairwise root mean-square deviation from experimental B-factors. *Biophys. J.* **2010**, *98*, 861–871.
- (38) Khan, M. T.; Chinnasamy, S.; Cui, Z.; Irfan, M.; Wei, D.-Q. Mechanistic analysis of A46V, H57Y, and D129N in pyrazinamidase associated with pyrazinamide resistance. *Saudi J. Biol. Sci.* **2020**, *27*, 3150–3156.
- (39) Nath, A.; Kumer, A.; Khan, M. W. Synthesis, computational and molecular docking study of some 2, 3-dihydrobenzofuran and its derivatives. *J. Mol. Struct.* **2021**, *1224*, No. 129225.
- (40) Ruud, K.; Helgaker, T.; Bouř, P. Gauge-origin independent density-functional theory calculations of vibrational Raman optical activity. *J. Phys. Chem. A* **2002**, *106*, 7448–7455.
- (41) Del Bene, J. E.; Person, W. B.; Szczepaniak, K. Properties of Hydrogen-Bonded Complexes Obtained from the B3LYP Functional with 6-31G (d, p) and 6-31+ G (d, p) Basis Sets: Comparison with MP2/6-31+ G (d, p) Results and Experimental Data. *J. Phys. Chem. A* **1995**, *99*, 10705–10707.
- (42) Schäfer, A.; Huber, C.; Ahlrichs, R. Fully optimized contracted Gaussian basis sets of triple zeta valence quality for atoms Li to Kr. *J. Chem. Phys. A* **1994**, *100*, 5829–5835.
- (43) Nath, A.; Kumer, A.; Zaben, F.; et al. Investigating the binding affinity, molecular dynamics, and ADMET properties of 2,3-dihydrobenzofuran derivatives as an inhibitor of fungi, bacteria, and virus protein. *Beni-Suef Univ. J. Basic Appl. Sci.* **2021**, *10*, No. 36.
- (44) Forli, S.; Olson, A. J. A Force Field with Discrete Displaceable Waters and Desolvation Entropy for Hydrated Ligand Docking. *J. Med. Chem.* **2012**, *55*, 623–638.
- (45) Land, H.; Humble, M. S. YASARA: A Tool to Obtain Structural Guidance in Biocatalytic Investigations. In *Protein Engineering*; Springer, 2018; pp 43–67.
- (46) Kandeel, M.; Al-Taher, A.; Li, H.; Schwingschlogl, U.; Al-Nazawi, M. Molecular dynamics of Middle East respiratory syndrome coronavirus (MERS CoV) fusion heptad repeat trimers. *Comput. Biol. Chem.* **2018**, *75*, 205–212.